JOURNAL OF
GENERAL VIROLOGY

RESEARCH ARTICLE
Graul *et al.*, *Journal of General Virology* 2019;100:497–510
DOI 10.1099/jgv.0.001224

MICROBIOLOGY SOCIETY

Transmembrane regions of bovine herpesvirus 1-encoded UL49.5 and glycoprotein M regulate complex maturation and ER–Golgi trafficking

Małgorzata Graul,[1] Edyta Kisielnicka,[1] Michał Rychłowski,[1] Marieke C. Verweij,[2] Kurt Tobler,[3] Mathias Ackermann,[3] Emmanuel J. H. J. Wiertz,[4] Krystyna Bieńkowska-Szewczyk[1] and Andrea D. Lipińska[1,*]

Abstract

Bovine herpesvirus 1 (BoHV-1)-encoded UL49.5 (a homologue of herpesvirus glycoprotein N) can combine different functions, regulated by complex formation with viral glycoprotein M (gM). We aimed to identify the mechanisms governing the immunomodulatory activity of BoHV-1 UL49.5. In this study, we addressed the impact of gM/UL49.5-specific regions on heterodimer formation, folding and trafficking from the endoplasmic reticulum (ER) to the *trans*-Golgi network (TGN) – events previously found to be responsible for abrogation of the UL49.5-mediated inhibition of the transporter associated with antigen processing (TAP). We first established, using viral mutants, that no other viral protein could efficiently compensate for the chaperone function of UL49.5 within the complex. The cytoplasmic tail of gM, containing putative trafficking signals, was dispensable either for ER retention of gM or for the release of the complex. We constructed cell lines with stable co-expression of BoHV-1 gM with chimeric UL49.5 variants, composed of the BoHV-1 N-terminal domain fused to the transmembrane region (TM) from UL49.5 of varicella-zoster virus or TM and the cytoplasmic tail of influenza virus haemagglutinin. Those membrane-anchored N-terminal domains of UL49.5 were sufficient to form a complex, yet gM/UL49.5 folding and ER–TGN trafficking could be affected by the UL49.5 TM sequence. Finally, we found that leucine substitutions in putative glycine zipper motifs within TM helices of gM resulted in strong reduction of complex formation and decreased ability of gM to interfere with UL49.5-mediated major histocompatibility class I downregulation. These findings highlight the importance of gM/UL49.5 transmembrane domains for the biology of this conserved herpesvirus protein complex.

INTRODUCTION

Bovine herpesvirus 1 (BoHV-1) is an important veterinary pathogen, causing ocular, respiratory and genital infections in cattle [1]. BoHV-1 is closely related to other alphaherpesviruses of veterinary importance, such as pseudorabies virus (PRV) or equine herpesvirus 1 (EHV-1), as well as human alphaherpesviruses, including human herpesvirus 3 [varicella-zoster virus (VZV)] or human herpesvirus 1 [herpes simplex virus 1 (HSV-1)], and it shares many properties of this group of viruses. Like other herpesviruses, BoHV-1 infection induces a strong host immune response, which is counteracted by viral proteins and microRNAs at various stages to enable the establishment of latency [2, 3]. A key player in the immune evasion strategies of BoHV-1 is the UL49.5 protein – the non-glycosylated glycoprotein N (gN) homologue.

UL49.5 is a small [96 amino acid (aa) residues for BoHV-1] type I transmembrane protein, which is conserved throughout the family *Herpesviridae*. It comprises a cleavable signal peptide, an N-terminal extracellular domain, a transmembrane region (TM) and a short C-terminal cytosolic tail [4, 5]. UL49.5 can be observed in the following two major forms: as a sole polypeptide (single chain and homodimeric) or in a complex with another conserved herpesvirus protein,

Received 26 February 2018; Accepted 3 January 2019; Published 29 January 2019
Author affiliations: [1]Laboratory of Virus Molecular Biology, Intercollegiate Faculty of Biotechnology, University of Gdańsk and Medical University of Gdańsk, Gdańsk, Poland; [2]Department of Medical Microbiology, Leiden University Medical Center, Leiden, The Netherlands; [3]Institute of Virology, University of Zurich, Zurich, Switzerland; [4]Department of Medical Microbiology, University Medical Center Utrecht, Utrecht, The Netherlands.
***Correspondence:** Andrea D. Lipińska, andrea.lipinska@biotech.ug.edu.pl
Keywords: alphaherpesviruses; bovine herpesvirus 1; UL49.5/glycoprotein M complex; transmembrane region; cytoplasmic domain; glycine zipper.
Abbreviations: BAC, bacterial artificial chromosome; BoHV-1, bovine herpesvirus 1; conA, concanavalin A; EEA1, early endosome antigen 1; EHV-1, equine herpesvirus 1; endoH, endoglycosidase H; ER, endoplasmic reticulum; gM, glycoprotein M; gN, glycoprotein N; HA, haemagglutinin; HCMV, human cytomegalovirus; HSV-1, herpes simplex 1 virus; IB, immunoblotting; IP, immunoprecipitation; Kan^R, kanamycin resistance; MAb, monoclonal antibody; MDBK, Madin–Darby bovine kidney; MHC, major histocompatibility complex; PAb, polyclonal antibody; PNGaseF, peptide:N-glycosidase F; PRV, pseudorabies virus; TGN, *trans*-Golgi network; TAP, transporter associated with antigen processing; TM, transmembrane; UL, unique long; US, unique short; VZV, varicella-zoster virus; WT, wild-type.
Supplementary material is available with the online version of this article.

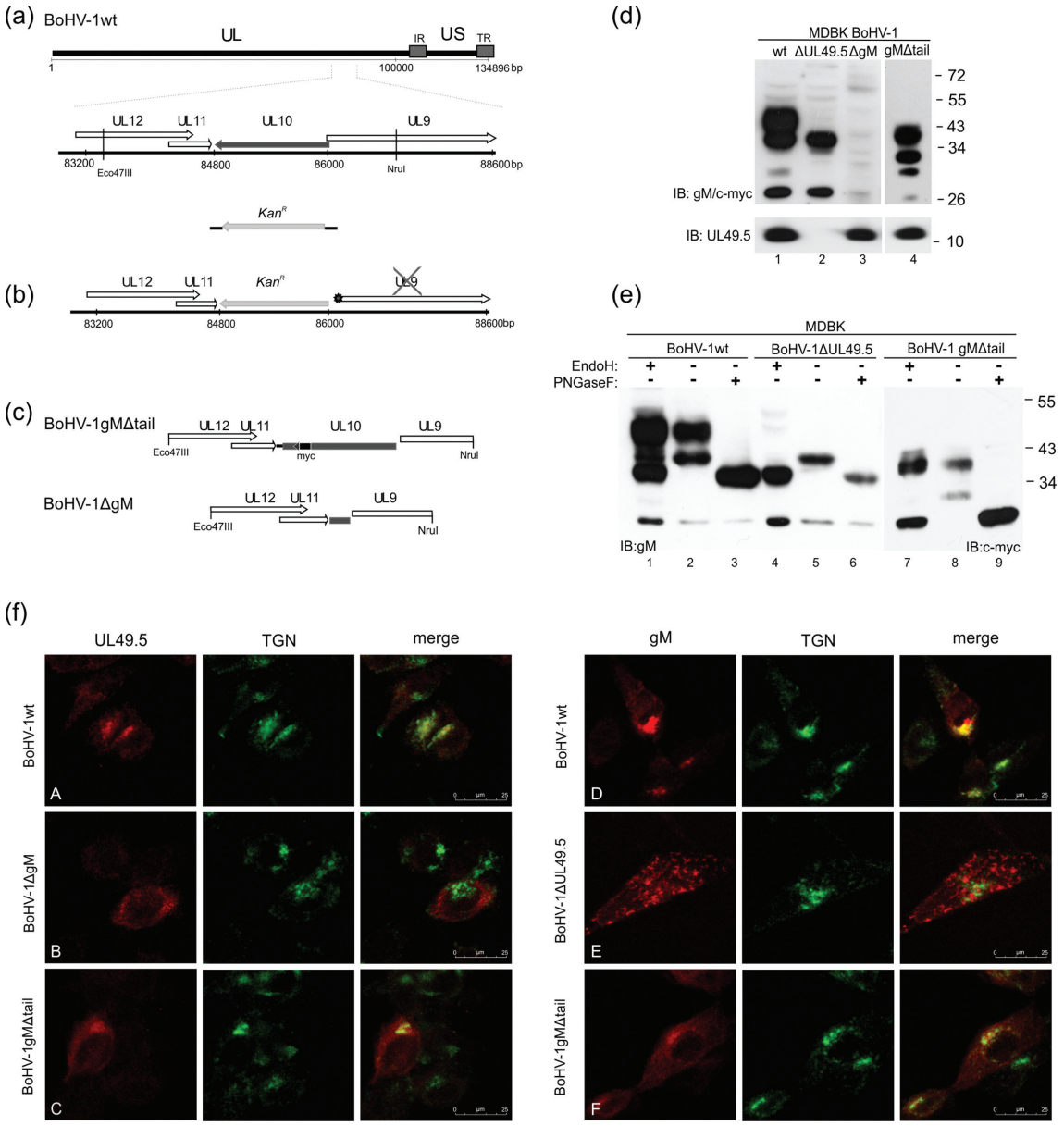

Fig. 1. The cytoplasmic domain of gM is dispensable for ER–Golgi trafficking of the UL49.5/gM complex during BoHV-1 infection. (a) Schematic arrangement of BoHV-1 genome and the cassette used for Red recombination and construction of BoHV-1 mutants. The genome is composed of unique long (UL) and unique short (US) regions flanked by internal repeats (IR) and terminal repeats (TR); the region between 83 200 and 88660 bp containing UL9, UL10 (gM gene) and UL11 is shown in detail. (b) Diagram of the replication-deficient BoHV-1 mutant containing the *Kan*^{R} gene in place of UL10 and disrupted UL9. (c) Homologous recombination cassette containing truncated UL10 fused to a c-myc tag (for BoHV-1gMΔtail) or gM deletion (for BoHV-1ΔgM). (d) Expression of gM and UL49.5 in MDBK cells infected for 24 h with the constructed BoHV-1 mutants was evaluated by immunoblotting using anti-gM, anti-c-myc (for BoHV-1 gMΔtail), or anti-UL49.5 antibodies. (e) Maturation of gM in MDBK cells infected with BoHV-1 mutants was investigated by endoglycosidase treatment. BoHV-1wt-, BoHV-1ΔUL49.5-, or BoHV-1gMΔtail-infected cell lysates were treated with EndoH (+) or PNGaseF (+), or left untreated (–), and then proteins were immunoblotted with anti-gM or anti-c-myc antibodies. (f) Subcellular localization of gM in BoHV-1-infected cells was evaluated by laser scanning confocal microscopy. MDBK cells were infected with BoHV-1wt (a, d) or its mutants – BoHV-1ΔgM (b), BoHV-1ΔUL49.5 (e), or BoHV-1gMΔtail (c, f) – at a multiplicity of infection (m.o.i.) of 0.6 for 14 h, and then the cells were fixed, permeabilized and stained with anti-γ-adaptin MAb (TGN marker, green) and either anti-gM (panels D–F) or anti-UL49.5 antibodies (panels A–C) (red).

glycoprotein M (gM), during BoHV-1 infection [6–8]. For the growth of BoHV-1 in *in vitro* cultures, both genes are nonessential [9, 10]. However, UL49.5 is an important virulence determinant. The gM-unbound form of UL49.5 acts as an inhibitor of the transporter associated with antigen processing (TAP), downregulating surface expression of major histocompatibility complex class I molecules (MHC I) [4, 7]. UL49.5 modifications also affect the antiviral immune response *in vivo* in mutant BoHV-1-infected calves [11]. Interestingly, the UL49.5 form acting on TAP should be regarded as 'immature', as it is retained by the endoplasmic reticulum (ER) quality control system. gM binding counteracts TAP inhibition, as it most probably sequesters the UL49.5 protein and facilitates proper folding of both viral polypeptides and the release of the complex to more distal compartments of the secretory pathway. We have previously shown that the cytosolic tail of UL49.5 is dispensable for these events [7].

Most herpesvirus UL49.5 homologues act as a chaperone for gM, and complex formation is required for proper processing and virion incorporation of most UL49.5 homologues [12–15], with the reported exceptions being in PRV and HSV-1 [16, 17]. gM, a product of the UL10 gene, is a highly hydrophobic type III transmembrane protein that is predicted to cross the membrane eight times. The BoHV-1 homologue codes for the 411 aa glycoprotein, with a conserved cysteine and a single N-glycosylation site located in the first extracellular domain, and potential trafficking motifs in the C-terminal cytosolic tail [8, 16]. Homologues of gM participate in diverse processes during herpesvirus infection, including the secondary envelopment of virus particles, egress and cell-to-cell spread [18–21]. The formation of BoHV-1, EHV-1 and human cytomegalovirus (HCMV) gM/UL49.5 complexes has been shown to rely on a disulfide bridge between the conserved cysteine residues [8, 17, 22]. However, stabilization of the gM/UL49.5 complex in HCMV and HSV-1 requires additional noncovalent interactions [23, 24]. In contrast, and despite the presence of conserved cysteines, VZV complex formation depends on a noncovalent interaction involving a valine residue at position 42 and a glycine at position 301 (seventh TM) forming a conserved tandem GxxxG motif, the so-called 'glycine zipper' [25]. There are increasing data on the role of single, tandem (glycine zippers) and extended GxxxG and GxxxG-like (with glycine replaced by other small amino acid residues such as alanine or serine) motifs located in the TM regions of cellular and viral proteins in granting the helix–helix proximity, facilitating helix–helix interactions between proteins or domains of a protein, and/or assisting in protein folding [26–29].

We explore the mechanisms that modulate UL49.5 activity, such as the interaction with gM, in our studies of BoHV-1 immune evasion. The present report is focused on the contribution of BoHV-1 UL49.5 and gM domains to heterodimer formation and maturation. We show that the transmembrane 'core' of the complex, encompassing the N-terminal domain of BoHV-1-encoded UL49.5, in concert with its TM region and the N-terminal-transmembrane domain of gM, is sufficient to bind, fold and be transported to the TGN. In addition, our data correlate the efficiency of gM/UL49.5 maturation with the sequence of the TM regions of UL49.5 and gM, especially the G219/A223/G227 and, to a lesser extent, G280/G284/A288 aa residues within the fifth and seventh TM helices of gM, respectively, forming putative glycine zippers. Our results highlight the importance of interactions within and between the transmembrane domains of BoHV-1 gM/UL49.5, which may be conserved in their herpesviral counterparts.

RESULTS

The cytoplasmic domain of gM is dispensable for ER–Golgi trafficking of the UL49.5/gM complex during BoHV-1 infection

When expressed individually, independently of infection, BoHV-1 gM and UL49.5 proteins are retained in the ER in their immature forms prior to complex formation. They seem to be the only viral factors required for the maturation of the complex, regarded as proper folding, release by the ER quality control system, and trafficking via the secretory pathway. Maturation is accompanied by the processing of the gM N-glycan, not excluding other potential modifications [7]. A BoHV-1 virus mutant lacking gM expression (BoHV-1ΔgM) was constructed by deleting codons 138–357, in order to evaluate the influence of other viral components on gM/UL49.5 processing during infection. Furthermore, we hypothesized that the C-terminal domain of gM would be the most probable source of motifs regulating its own trafficking and that of the whole complex. Scanning of the gM sequence for conserved motifs revealed the presence of a di-acidic EGD (aa 379–381) motif and a polybasic signal HHRRK (aa 343–347), which may resemble the arginine-based ER retention motifs. Its membrane-proximity suggests, however, that it could act as an ER export determinant [30, 31]. We have previously shown that the short cytoplasmic tail of UL49.5 is not required for UL49.5 retention or release of the complex when bound to gM [7]. Therefore, we constructed a BoHV-1 mutant producing tailless gM, lacking 71 most C-terminal aa residues (BoHV-1gMΔtail). The mutants were generated with the use of a BoHV-1 strain Jura clone as a bacterial artificial chromosome (BAC) [32] in a two-step strategy. First, taking advantage of the fact that UL10 gene is neighboured by the essential UL9 sequence [33] (Fig. 1a), UL10 was replaced in bacteria by the kanamycin resistance marker (Kan^R) gene, disrupting the UL9 expression and resulting in a replication-deficient BoHV-1 mutant (Fig. 1b). In the second step, Kan^R was replaced by the ΔgM or gMΔtail cassette, which also restored UL9 expression (Fig. 1c). To enable detection of gMΔtail, a c-myc tag was introduced at the C-terminus of the protein. BoHV-1ΔgM and BoHV-1gMΔtail grew with similar kinetics to the parental BoHV-1 Jura strain, but produced plaques that were on average 30 and 25% smaller,

respectively (Fig. S1, available in the online version of this article).

Expression of the two proteins was analysed in MDBK cells infected with BoHV-1wt, BoHV-1ΔgM, or BoHV-1ΔUL49.5 (obtained in our previous study [10]) by immunoblotting, in order to investigate the interdependence of BoHV-1 gM and UL49.5 processing during infection. No UL49.5 protein could be detected in cells infected with BoHV-1ΔUL49.5 and no gM expression was observed in cells infected with BoHV-1ΔgM (Fig. 1d, lanes 2 and 3), as expected, while the UL49.5 levels in cells infected with BoHV-1wt and BoHV-1ΔgM were comparable. In lysates of MDBK cells infected with BoHV-1wt, the previously characterized [7] major gM forms could be detected, with molecular masses of 45, 36 and 34 kDa. An additional 26 kDa band may represent a cleaved C-terminal fragment. gM from cells infected with BoHV-1ΔUL49.5 migrated predominantly as lower-molecular-mass bands. Based on the sensitivity of its N-glycan to endoglycosidases, the maturation status of gM was evaluated. PNGaseF treatment, which removes all N-glycans, identified the 34 kDa gM band as the non-glycosylated precursor (Fig. 1e, lanes 2 and 3). The high-molecular-mass form was resistant to endoglycosidase H (endoH); thus, it presumably represented the fully N-glycosylated gM, which has reached the TGN (Fig. 1e, lanes 1 and 2). The 36 kDa band shifted upon endoH; hence, it shou/ld represent the immature, ER-*cis* Golgi-resident gM. This form dominated in BoHV-1ΔUL49.5-infected cells, with no obvious endoH-resistant gM production. Immunoblotting analysis of BoHV-1gMΔtail-infected MDBK lysates was able to demonstrate three forms of gM, with molecular masses of 38, 32 and 29 kDa (Fig. 1d, lane 4). The PNGaseF and endoH analyses identified them as both endoH-sensitive (32 kDa) and endoH-resistant (38 kDa) proteins, with the 29 kDa form most probably representing the tailless gMΔtail precursor (Fig. 1e, lanes 7–9).

Maturation of UL49.5 was analysed by showing its subcellular localization with the use of immunofluorescence confocal laser scanning microscopy. While in cells infected with BoHV-1wt the UL49.5 protein (Fig. 1f, and gM could be detected both perinuclearly (resembling ER membranes) and in colocalization with the TGN marker γ-adaptin (Fig. 1f, panels A and D), neither of the two proteins showed a clear TGN localization when expressed without the partner (Fig. 1f, panels B and E). The co-localization was additionally analysed using Leica software, with a Pearson's correlation coefficient of 0.356 being obtained for the TGN and UL49.5 signal overlay in BoHV-1ΔgM-infected cells and one of 0.341 being obtained for TGN and gM co-localization in BoHV-1ΔUL49.5-infected cells – neither value reached the threshold of 0.5, which is regarded as indicating significant co-localization. Interestingly, in cells infected with BoHV-1ΔUL49.5 (Fig. 1f, panel E), gM demonstrated a granular localization pattern, which may indicate the presence of aggregates of misfolded glycoprotein. In MDBK cells infected with BoHV-1gMΔtail, both UL49.5 (Fig. 1f, panel E) and gMΔtail (Fig. 1f, panel F) partially co-localized with the TGN marker γ-adaptin. Taken together, these results demonstrate that UL49.5 and gM are necessary and sufficient for their maturation as a complex during BoHV-1 infection and no other viral component can efficiently compensate for this chaperone function. In addition, the cytoplasmic tail of gM was dispensable for the ER release and maturation of the glycoprotein produced in the presence of UL49.5.

The cytoplasmic domains of BoHV-1 UL49.5 and gM are dispensable for complex formation and ER release in stable cell lines

To investigate the role of gM/UL49.5 cytoplasmic domains in more detail, tailless gM was co-expressed with tailless UL49.5 (aa 1–80) in stable human melanoma MJS cell lines transduced with retroviral vectors and sorted for high purity and similar expression of marker genes (MJS UL49.5Δtail gMΔtail). The previously described [7] full-length protein-producing cells (MJS UL49.5 gM) or MJS UL49.5Δtail gM served as controls. Both gM variants were c-myc-His-tagged to facilitate the detection. As confirmed by immunoblotting (Fig. 2a), the UL49.5 expression levels were comparable in those cell lines. We were able to visualize gM forms with shifts of approximately 4 kDa in molecular masses, in comparison to the BoHV-1wt/BoHV-1 gMΔtail-infected cells. Those higher molecular masses of gM can be at least partially explained by the incorporation of c-myc and His tags, with two short aa linkers derived from the cloning procedure, into the C-terminus of our constructs, or the effect of those aa sequences on the migration of gM in SDS-PAGE gels. Of note, gMΔtail was detected in lower amounts than gMwt. We cannot explain this observation based on the obtained data. One possible explanation could be enhanced proteasomal degradation of tailless gM, yet its levels failed to be rescued with the proteasomal inhibitor MG132 (data not shown).

Both UL49.5wt and gMwt co-expressed in MJS cells co-localized with each other, as well as with the TGN marker γ-adaptin (Fig. 2b, panel A). Partial overlapping with the ER-*cis* Golgi marker concanavalin A (Fig. 2b, panel B) could also be detected. Co-localization of both viral proteins and their TGN or ER localization (Fig. 2b, panels C and D) were not disrupted by the deletion of the cytoplasmic tail of UL49.5. gMΔtail, when co-expressed with UL49.5 or UL49.5Δtail, was released from the ER and transported via the secretory pathway. In addition to the TGN and ER localization, it could be detected beyond these compartments, including the plasma membrane (Figs 2b, panels E–H and S2). Higher plasma membrane levels of UL49.5/UL49.5Δtail in the presence of gMΔtail could also be detected by flow cytometry (Fig. S2). The tailless gM and co-expressed UL49.5 could additionally be found in early endosomes. The distribution of EEA1-positive endosomes in those cells seemed to be altered, as the EEA1 marker and the BoHV-1 proteins showed a more clustered co-localization pattern (Fig. S2). The

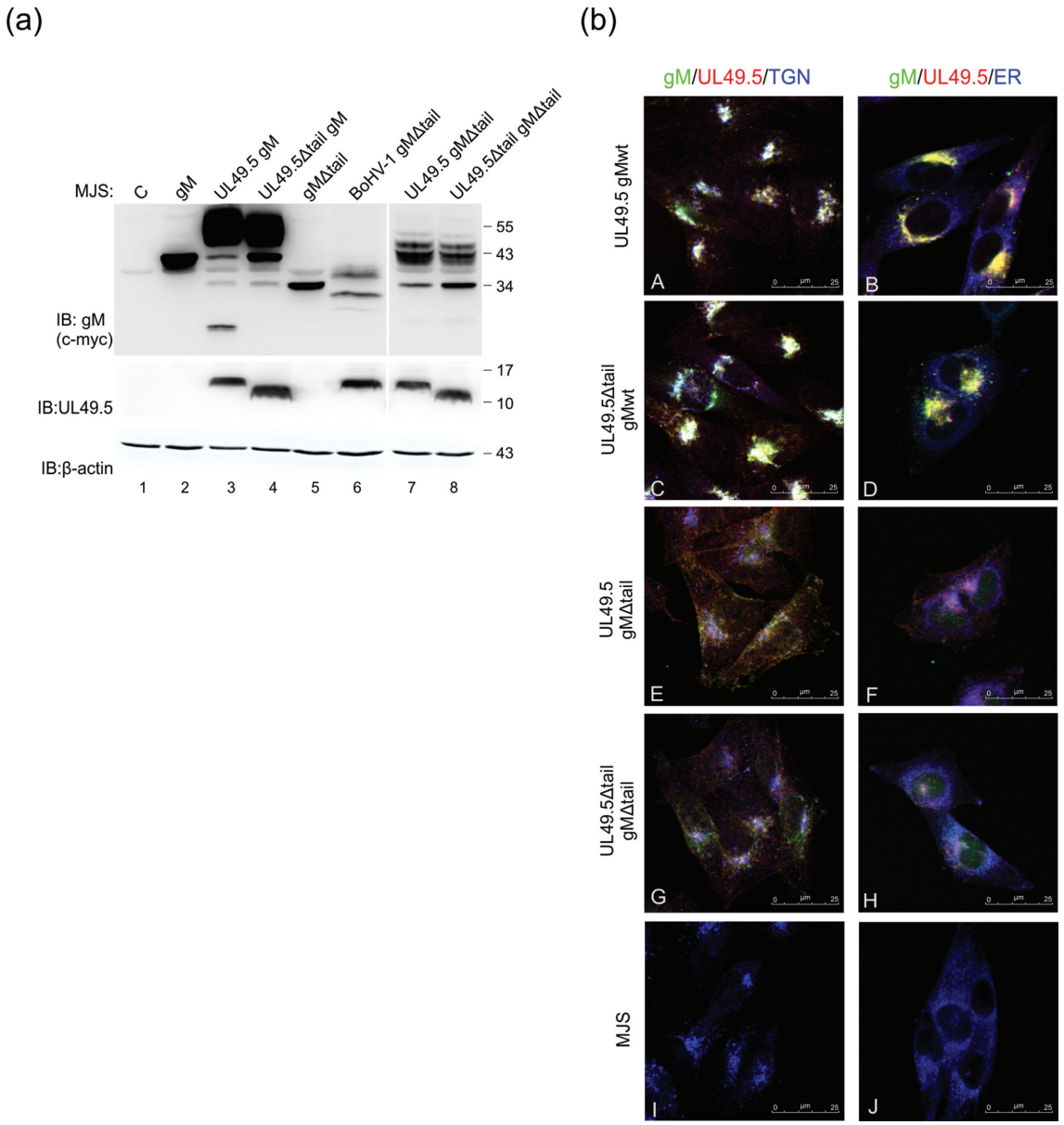

Fig. 2. The cytoplasmic domains of BoHV-1 UL49.5 and gM are dispensable for complex formation and ER release. (a) Expression and maturation of constructed tailless forms of gM and UL49.5 in MJS cell lines were evaluated using SDS-PAGE followed by immunoblotting (IB). gM was detected with anti-c-myc antibodies and UL49.5 was detected using anti-UL49.5 antibodies. β-actin was used as a loading control. (b) Subcellular localization of investigated proteins in MJS cell lines was evaluated by immunofluorescence laser scanning confocal microscopy. The cells in panels A, C, E, G and I were stained with goat anti-c-myc (for gM, green), rabbit anti-UL49.5 (red) and anti-γ-adaptin antibodies (for TGN, blue). The cells in panels B, D, F, H, J were stained with goat anti-c-myc (for gM, green), rabbit anti-UL49.5 antibodies (red) and Alexa 633-conjugated concanavalin A (ConA, blue) to visualize ER.

immunofluorescence analysis supports the conclusion that the C-terminal tail of gM is not responsible for gM retention in the ER or ER–Golgi trafficking of UL49.5/gM, but it may influence the localization of the complex in other compartments. Since the cytoplasmic tail of gM also contains potential conserved endocytosis motifs [such as the tyrosine-based YGHV (aa 352–355), acidic cluster DDEE (aa 393–396) and dileucine (aa 385–386)] sequences, most likely the tailless gM/UL49.5 remains at least partially retained in the plasma membrane.

The transmembrane domain of BoHV-1 UL49.5 is required for proper gM/UL49.5 complex maturation

While exploring the role of UL49.5 domains in the inhibition of TAP [34], we were previously able to show that the N-terminal domain of UL49.5 was highly unstable when

expressed alone, and it required a membrane anchor to bind TAP and inhibit MHC I. The sequence of TM could, however, affect the stability of UL49.5 and, possibly, interaction with TAP proteins. We used the same approach with chimeric UL49.5 variants, co-expressed with gM in stable MJS cells (Fig. 3a), in order to test whether this is also true for the interaction of UL49.5 with gM. The first chimera ($BoHV_N$-VZV_{TM}) was composed of the N-terminal domain from BoHV-1 UL49.5 and the TM region from a related varicella-zoster (VZV) UL49.5 homologue (ORF9A in VZV-specific gene nomenclature). VZV UL49.5 was selected as a TM 'donor' due to its close relation to BoHV-1 and potential structural resemblance [10]. No significant variations in the steady-state levels of UL49.5 variants were detected in lysates of MJS co-expressing gM with $BoHV_N$-VZV_{TM} UL49.5 or BoHV-1 UL49.5Δtail (Fig. 3b). The N-glycosylation status of BoHV-1-encoded gM expressed in the presence of the investigated UL49.5 chimera was evaluated by endoglycosidase treatment and immunoblotting (Fig. 3c). The following two forms of gM could be detected in the presence of the $BoHV_N$-VZV_{TM} UL49.5: a 55 kDa EndoH-resistant and a 42 kDa EndoH-sensitive band. The level of gM with a fully processed N-glycan in those cells was much lower than in the wild-type BoHV-1 UL49.5-producing cells, which indicates that gM maturation in the complex is at least partially impaired when UL49.5 lacks its original TM.

Next, the ectodomain of UL49.5 was fused to a heterologous transmembrane region. In order to construct a chimeric $BoHV_N$-HA_{TM+C} UL49.5 protein (Fig. 3a), we used the TM of influenza haemagglutinin (HA). A 13 aa-long cytosolic tail of HA was added to this construct, as the incorporation of the HA TM alone resulted in a protein with reduced stability (data not shown). $BoHV_N$-HA_{TM+C} UL49.5 was expressed at levels that were still lower than those for UL49.5Δtail (Fig. 3d, lower panel, compare lanes 2 and 4) and its stability could be increased with the proteasomal inhibitor MG132 (Fig. 3d, lower panel, lane 5). However, even in the presence of MG132-stabilized $BoHV_N$-HA_{TM+C} UL49.5, high-molecular-weight gM could hardly be detected (Fig. 3d, upper panel, lane 5). Co-immunoprecipitation (co-IP) was performed in order to assess whether the N-terminal domain of UL49.5 fused to a heterologous anchor could still bind gM. UL49.5 could be found in the complexes precipitated by anti-c-myc (for gM) antibodies, with the immature gM form and minute amounts of high-molecular-weight gM (Fig. 3e). This result may indicate that the chimeric protein interacts predominantly with the immature gM, whose further processing seems to be impaired.

Immunofluorescence confocal laser scanning microscopy analysis of the subcellular localization of chimeric proteins and gM demonstrated clear co-localization of $BoHV_N$-VZV_{TM} UL49.5 and gM with the TGN marker, although it seems that slightly fewer viral proteins were able to reach TGN, when compared to the wild-type UL49.5 and gM. More $BoHV_N$-VZV_{TM} and co-expressed gM could be detected, instead, in the ER (Fig. S3). In the case of $BoHV_N$-HA_{TM+C} UL49.5, only minor amounts of both gM and the UL49.5 chimera co-localized in the TGN, whereas their ER co-localization was intensive (Fig. S3). Altogether, these data may suggest that the anchored N-terminal domain of UL49.5 is competent to form a complex with gM, but not sufficient for its efficient maturation. Therefore, it seems that the sequence of UL49.5 TM can influence processes resulting in the release of the gM/UL49.5 complex from the ER/*cis*-Golgi.

The tandem GxxxG-like motifs (G219A223G227 and G280/G284/A288) in BoHV-1 gM are required for the ER release and maturation of the gM/UL49.5 complex

Looking for specific motifs in the TM regions of UL49.5 and gM, the aa sequences of TM were compared between several alphaherpesvirus homologues (Fig 4). We selected the following three putative GxxxG or GxxxG-like (when alanine residue substitutes glycine) motifs within BoHV-1 gM that could be involved in the interaction with UL49.5: G20/A24 residues that create a single GxxxG-like (GVFAA) motif located in the first TM of gM, G219/A223/G227 residues that constitute a tandem GGLLALIIG motif in the fifth TM of gM and G280/G284/A288 residues that create a tandem GPAFGTLVA motif in the seventh TM of gM. The latter is homologous to the functional glycine zipper motif of VZV gM [25]. The TM of UL49.5 has a conserved AVMVA motif; thus, we selected A65 and A69 as potential involved residues. As small residues can substitute in glycine zipper motifs, selected glycine/alanine residues were replaced by leucine residues. This approach is commonly used in GxxxG studies to disrupt potential helix–helix interactions. It resulted in the construction of gMGAG/LLL (G219LA223LG227L), gMGA/LL (G20LA24L), gMGGA/LLL (G280LG284LA288L) and UL49.5AA/LL (A65LA69L). The constructs were, using retroviral vectors, constitutively expressed in MJS cells (sorted for >95 % purity) and the steady-state levels of the gM and UL49.5 variants were evaluated by immunoblotting (Fig. 5a). To facilitate detection, a c-myc tag was introduced at the C-terminus of the new gM variants. The expression levels of gMGA/LL (1 st TM) were slightly elevated in comparison to gMwt, nevertheless gM maturation seemed not to be altered, so this variant was not investigated further (Fig. 5a, lane 5). In the lysates of gMGAG/LLL (5th TM) and UL49.5wt co-expressing cells, only the immature form of gM could be detected, suggesting that this motif was crucial for gM maturation (Fig. 5a, lane 7). Compared to gMwt, gMGAG/LLL expression was slightly reduced. A similar effect of substitutions could be observed for gMGGA/LLL (7th TM), where gM maturation in cells co-expressing UL49.5 seemed to be impaired as well, resulting in a smaller proportion of the higher-molecular-weight gM band (Fig. 5a, lane 9). gM maturation was not disrupted in MJS-producing gMwt and UL49.5AA/LL, bringing into question the importance of the UL49.5 AxxxA motif (Fig. 5a, lane 11).

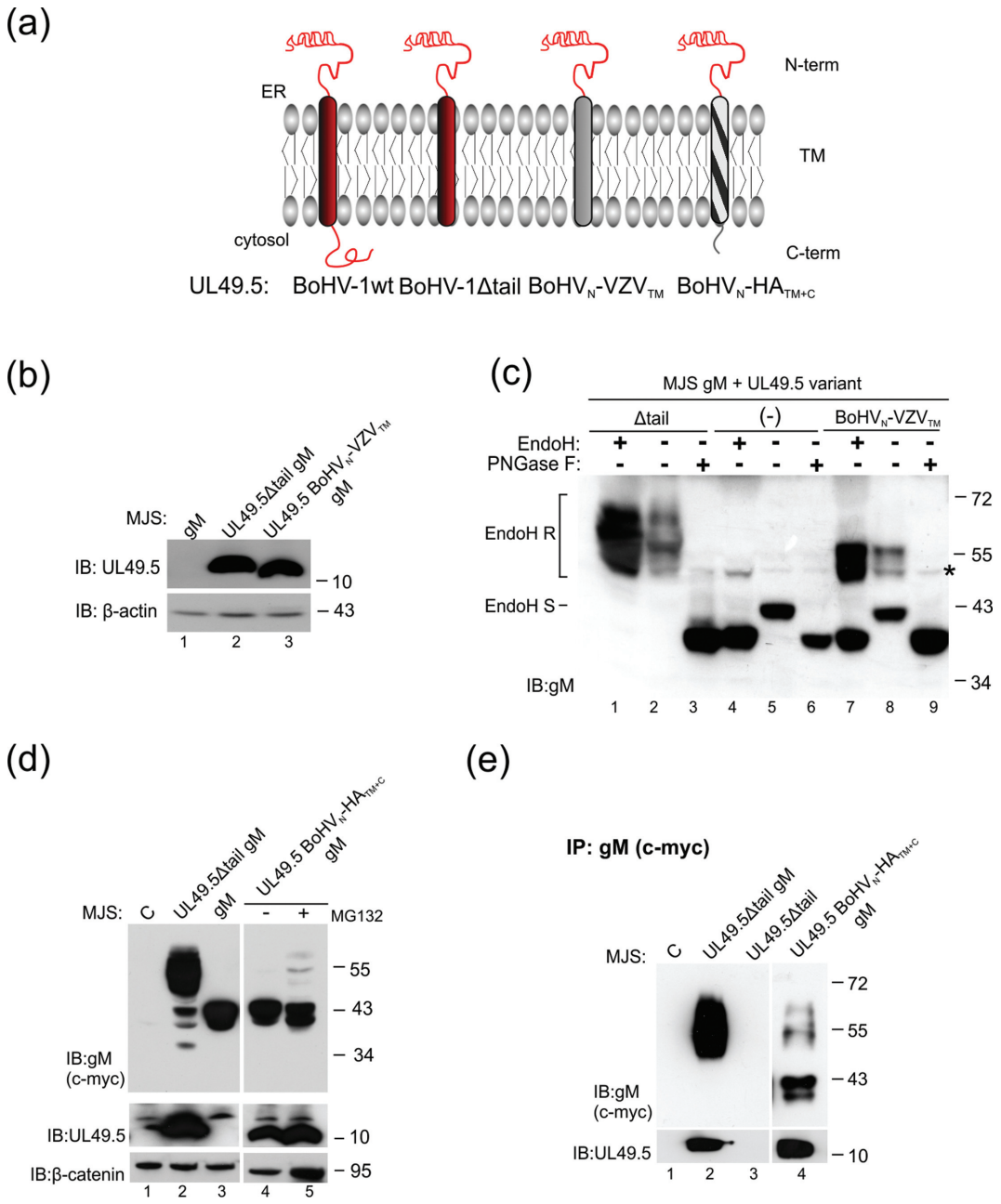

Fig. 3. The transmembrane domain of BoHV-1-encoded UL49.5 is required for proper complex maturation. (a) Schematic representation of constructed UL49.5 chimeras. BoHV-1wt is a full-length UL49.5 protein. BoHV-1Δtail is deprived of the cytoplasmic tail. The BoHV$_N$-VZV$_{TM}$ chimera is composed of the BoHV-1 N-terminal domain of UL49.5 and the TM of VZV UL49.5. BoHV$_N$-HA$_{TM+C}$ contains the N-terminal domain of BoHV-1 UL49.5 and the TM region of influenza haemagglutinin, together with its short cytosolic tail. (b) Expression of BoHV$_N$-VZV$_{TM}$ UL49.5 in stable MJS cell line was assessed by SDS-PAGE and immunoblotting (IB) using antibodies specific for BoHV-1 UL49.5. β-actin was detected as a loading control. (c) Maturation of gM in the presence of BoHV$_N$-VZV$_{TM}$ UL49.5 was evaluated by endoglycosidase treatment, followed by SDS-PAGE and IB using anti-gM antibodies. MJS cell lysates were treated with EndoH (+) or PNGaseF (+), or left untreated (–). *, unspecific staining of antibodies. (d) Expression of gM and BoHV$_N$-HA$_{TM+C}$ UL49.5 in a stable MJS cell line was analysed by IB using anti-c-myc (for gM) or BoHV-1 UL49.5-specific antibodies. The chimeric UL49.5 was additionally stabilized with the proteasomal inhibitor MG132. β-catenin was detected as a loading control. (e) Complex formation by BoHV$_N$-HA$_{TM+C}$ UL49.5 (MG132-stabilized) and gM was evaluated by co-IP using anti-c-myc antibodies. Immunoprecipitated proteins were separated by SDS-PAGE and detected with anti-c-myc (for gM) or anti-UL49.5 antibodies.

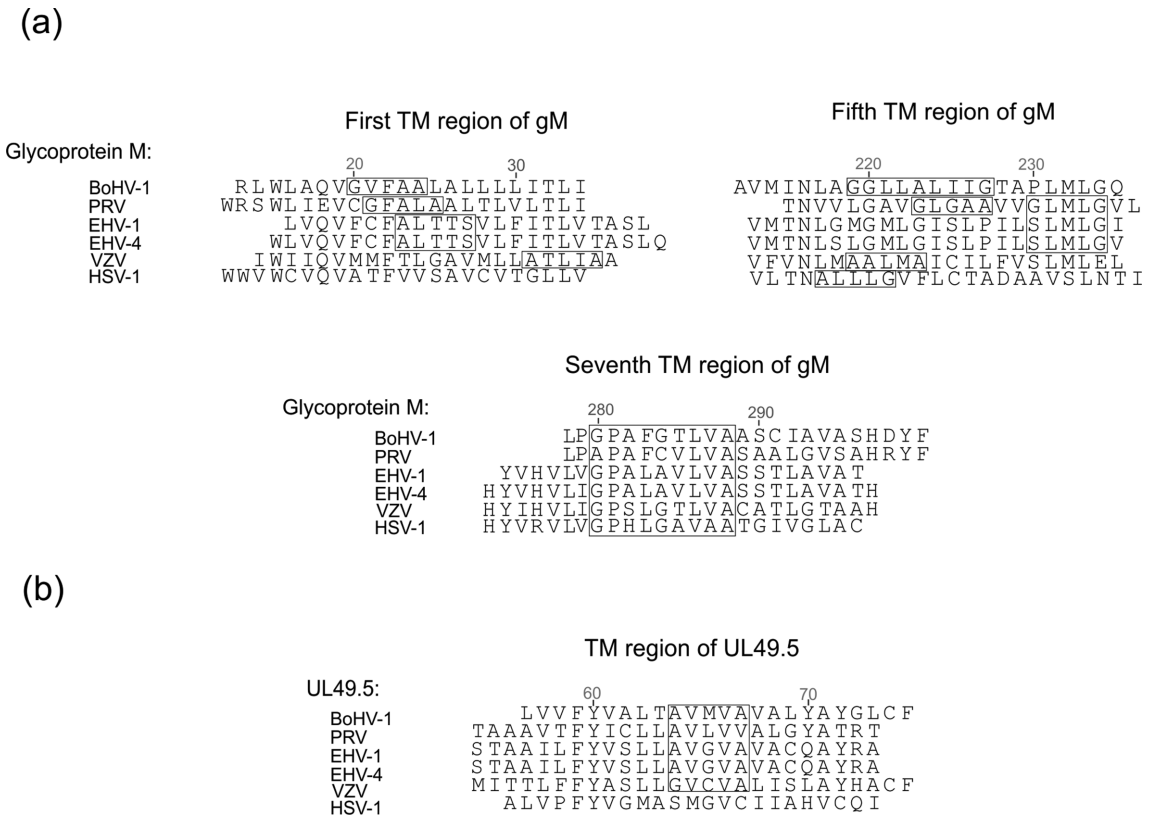

Fig. 4. Alignment of alphaherpesvirus-encoded transmembrane regions of gM and UL49.5 proteins. (a) Amino acid sequences of gM homologues were aligned using Geneious software. TM regions of gM homologues were predicted using TMHMM software (www.cbs.dtu.dk/services/TMHMM-2.0). Numeration indicates the position of aa residues in BoHV-1-encoded gM. (b) Amino acid sequences of UL49.5 TM were aligned using Geneious software. The boxes indicate potential GxxxG or GxxxG-like motifs located in TM regions.

At this stage, a gM mutant with a single leucine substitution of the central alanine residue in the G219/A223/G227 motif was also constructed, in order to ensure that our observations result from the impairment of the putative glycine zipper and not a general structural defect caused by the mutations. Stable, sorted MJS cell lines, expressing the gMA223L variant either alone, as a control, or co-expressing it with UL49.5, were obtained and analysed by immunoblotting. No mature gMA223L could be detected in the presence of UL49.5, just like in the case of the triple GAG mutant (Fig. 5b, lane 5).

The release of UL49.5 protein from the ER in the constructed cell lines was studied by immunofluorescence confocal laser scanning microscopy. UL49.5AA/LL could be detected with the co-expressed gMwt in the TGN (Fig. 5c, panel A), and the same could be observed for UL49.5wt co-expressed with gMGGA/LLL (Fig. 5c, panel B). Co-localization with UL49.5wt and the TGN marker was strongly reduced for gMGAG/LLL (Fig. 5c, panel C) and gMA223L (Fig. 5c, panel D). The latter two gM variants and UL49.5 showed more ER distribution (Fig. 5c, panels G and H). The presented data indicate that gM residues G219, A223 and G227 are especially important for the release of the gM/UL49.5 complex from the ER.

Co-IP analysis was performed in order to further investigate the role of the GAG and GGA motifs of gM and the AxxxA motif of UL49.5 in the complex formation (Fig. 5d). Efficient binding could be demonstrated for both the UL49.5 leucine substitution mutant (precipitated with gMwt, Fig. 5d, lane 6) and the GGA mutant of gM (interacting with UL49.5wt, Fig. 5d, lane 4). Interestingly, in comparison to the control, gMGAG/LLL and gMA223L co-precipitated UL49.5wt at a severely reduced level (Fig. 5d, lanes 3 and 5).

Putative glycine zipper gM mutant-UL49.5 interaction was also analysed by a non-reducing SDS-PAGE and immunoblotting with either anti-UL49.5 (Fig. 5e, left panel) or anti-gM (Fig. 5e, right panel) antibodies, demonstrating the importance of the G219/A223/G227 residues for complex formation even more clearly. In the case of gMwt/UL49.5-expressing cells, we observed a wide protein band with an average apparent molecular mass of 65 kDa, most probably representing the heterodimer (Fig. 5e, lanes 2 and 8). The gMGAG/LLL-UL49.5 complex was undetectable using this method (Fig. 5e, lanes 4 and 10). Monomeric UL49.5,

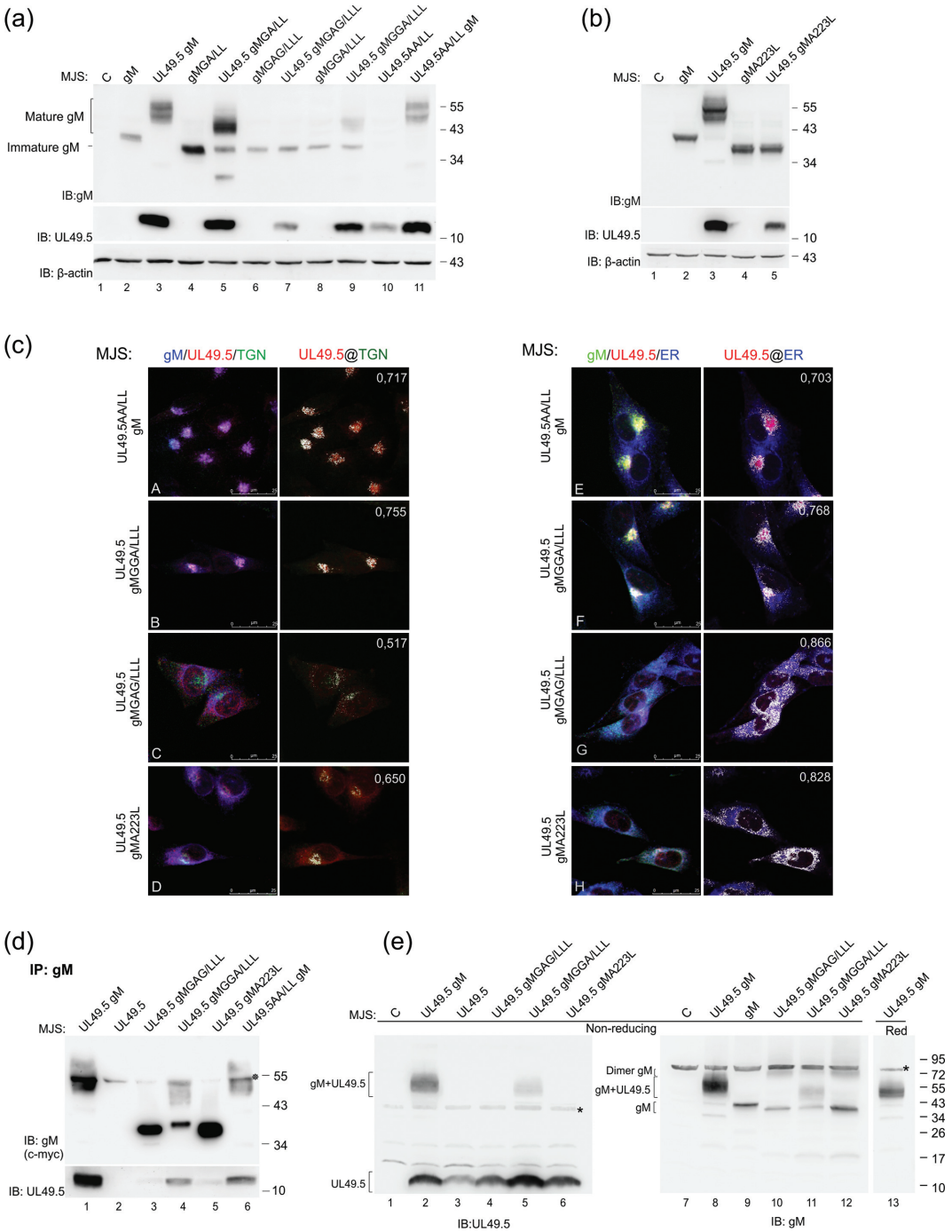

Fig. 5. Impact of mutations in GxxxG motifs of gM and UL49.5 on ER release and maturation of the gM/UL49.5 complex. (a) Expression and maturation of constructed gM and UL49.5 variants in stable MJS cell lines were evaluated by immunoblotting with anti-gM and anti-UL49.5 antibodies. β-actin was detected as a loading control. (b) Immunoblotting analysis of a single gMA223L mutant with anti-gM antibodies. UL49.5 was analysed in the cell lysates with UL49.5-specific antibodies and β-actin was detected as a loading control. (c) Subcellular localization of investigated proteins was evaluated by immunofluorescence laser scanning confocal microscopy. TGN (panels A–D) localization (green) was analysed using anti-γ-adaptin MAb together with goat anti-c-myc (for gM, blue) and rabbit anti-UL49.5 (red) antibodies. ER localization (panels E–H) was analysed with Alexa-633-conjugated ConA (blue) together with anti-c-myc MAb (for gM, green) and rabbit anti-UL49.5 antibodies (red). Merged images of UL49.5 and TGN or ER signals are shown in separate panels (UL49.5@TGN, UL49.5@ER), co-localization is depicted in white and the Pearson's correlation coefficient is included. (d) The ability of BoHV-1 gM/UL49.5 mutants to form a complex was assessed by co-IP using anti-gM antibodies. Immunoprecipitated proteins were separated by SDS-PAGE and stained with anti-c-myc (for gM) or anti-UL49.5 antibodies. The heavy chain of IgG used for IP is indicated by an asterisk (*). (d) Complex formation by gMGAG/LLL, gMA223L and gMGGA/LLL was analysed by a non-reducing SDS-

PAGE and immunoblotting with anti-UL49.5 (left panel) or anti-gM (right panel) antibodies. gM/UL49.5 cell lysate analysed in reducing conditions (red) was included in lane 13 for comparison.

monomeric gM, and, most probably, homodimeric gM also could be detected in the analysed samples, in the case of gMwt/UL49.5 – in addition to the heterodimer. The gMA223L protein preserved the properties of the triple mutant, and its ability to form a complex with UL49.5 was severely impaired (Fig. 5e, lanes 6 and 12). These results provide further evidence that the functional G219/A223/G227 motif of gM is required for efficient complex formation with UL49.5. A small amount of the heterodimer could be detected for the gMGGA/LLL variant (Fig. 5e, lanes 5 and 11), implying that this mutant exhibited an intermediate phenotype.

UL49.5-mediated MHC class I downregulation in the presence of gM G219LA223LG227L, A223L and G280LG284LA288L mutants

MHC I expression on MJS cells harbouring UL49.5 and gMGAG/LLL, gMA2323L, or gMGGA/LLL was assessed by flow cytometry (Fig. 6a), in order to study the functional consequences of mutations in the putative glycine zippers for gM-mediated regulation of UL49.5 activity toward TAP and surface MHC class I. In addition, the levels of the TAP1 and TAP2 subunits of the antigenic peptide transporter were analysed by immunoblotting (Fig. 6b) in the lysates of gMGAG/LLL co-expressing cells (as exhibiting the strongest effect of the mutation). gMwt co-expression partially 'rescues' MHC I surface expression and TAP protein levels [7]; for gMGAG/LLL, this ability was strongly impaired (in Fig. 6a compare the bold black and purple histograms). In the case of TAP degradation, it seemed to be as efficient in gMGAG/LLL-expressing cells as it was in non-gM-expressing cells (Fig. 6b, compare lanes 2 and 3). gMA223L failed to counteract UL49.5-mediated downregulation as well (Fig. 6a, red histogram), whereas the ability of gMGGA/LLL to rescue MHC I seemed to be intermediate (blue histogram in Fig. 6a).

DISCUSSION

BoHV-1-encoded gM appears to be a regulator of the immunomodulatory properties of UL49.5 at the stage of ER-associated folding and ER exit, and we show here that the transmembrane domains of both viral proteins have an impact on those events.

Our results indicate that UL49.5 and gM are interdependent for maturation during BoHV-1 infection, and no other viral protein can efficiently substitute for this chaperone function. In this respect, BoHV-1 gM/UL49.5 resemble most of their herpesvirus counterparts, described in the introduction. Such gM/UL49.5 complexes should be recognized as

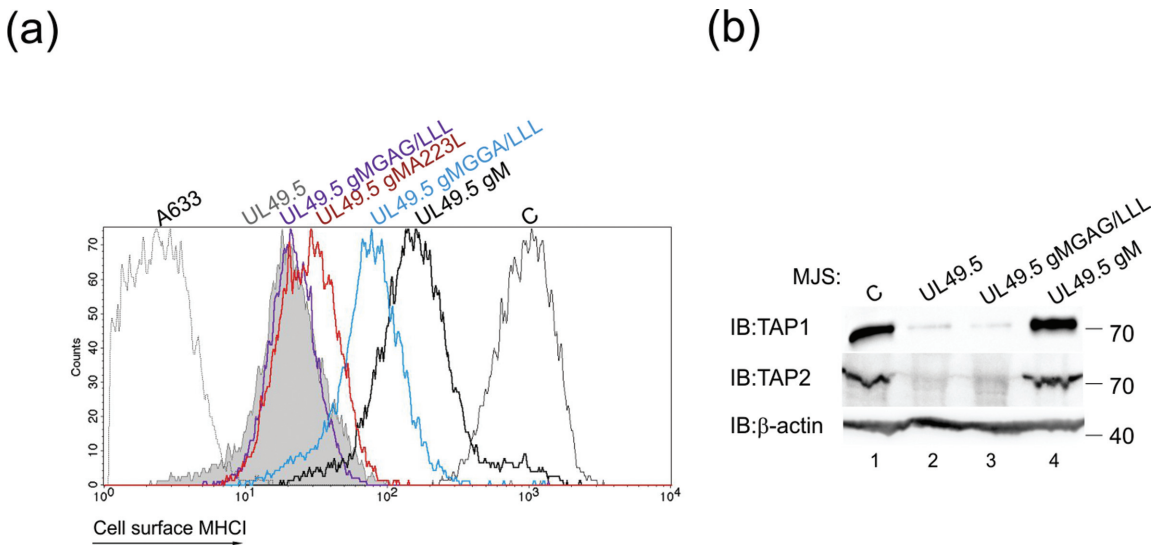

Fig. 6. UL49.5-mediated MHC class I downregulation in the presence of gM G219LA223LG227L, A223L and G280LG284LA288L mutants. (a) Surface expression of MHC class I on MJS cells expressing UL49.5 alone or together with gMwt, gMGAG/LLL, gMA223L, or gMGGA/LLL was analysed by flow cytometry. MHC I on surface of untransduced MJS cells was stained as a control (C); the A633 histogram represents the secondary antibody staining negative control. (b) Levels of TAP1 and TAP2 subunits in lysates of MJS cells expressing UL49.5 alone or together with gMwt or gMGAG/LLL were evaluated by IB with specific antibodies. β-actin was detected as a loading control.

one functional entity. There are several mechanisms leading to ER retention/ER retrieval of proteins, both signal-dependent and signal-independent (reviewed in [35, 36]). The cytoplasmic tail of gM appeared to us as the most probable source of trafficking signals. The other potentially important domain could be the N-terminus of gM, although this is less likely, as shown for homologous HSV-1 gM [37]. The fact that there is no significant impact of gM cytoplasmic tail removal on gM/UL49.5 complex formation and its ER–Golgi trafficking implis that ER retention of the two BoHV-1 proteins results rather from their misfolding and confinement by the chaperones of the ER quality control system. Similar results have been reported for HSV-1-encoded gM [24, 38], where the cytoplasmic tail of glycoprotein was dispensable for the ER–TGN transport. HSV-1 gM can, however, fold properly and reach the TGN independently of UL49.5, which makes for an important difference between the two homologues. The cytoplasmic tail of gM most probably contains motifs that are important for sorting to other subcellular compartments. It is difficult to visualize the full-length BoHV-1 gM in the plasma membrane, most probably because, like its herpesvirus homologues, it undergoes extensive endocytosis/retranslocation to the TGN. Detection of gMΔtail in higher amounts in the plasma membrane may suggest impaired endocytosis due to the removal of conserved endocytosis motifs located in the cytoplasmic tail. On the other hand, wild-type gM and UL49.5 were hardly detectable in early endosomes, in which gM resembles the VZV-encoded glycoprotein [20]. Increased co-localization of gMΔtail and co-expressed UL49.5 in early endosomes, showing at the same time a more clustered distribution, may indicate that the tail contains motifs governing endosomal trafficking of the complex. There are also other functions of gM and UL49.5, which may be determined by heterodimer formation and its transport, such as the control of membrane fusion events and cell-to-cell spread. BoHV-1 gM alone, in transient transfection experiments, could not inhibit bovine respiratory syncytial virus F protein-mediated cell fusion [9], and one possible explanation for this might be that its anti-fusogenic activity requires complex formation. The reduced plaque size resulting from gM (or its tail) deletion was, in fact, the only manifested impairment of the constructed virus mutants in *in vitro* cell cultures. While this paper was being revised, a report by Pannhorst *et al.* was published [39] in which the authors analysed the role of BoHV-1 gM and UL49.5 cysteine residues in the complex formation and looked for the functional significance of the UL49.5/gM complex. Some of our results are in line with their findings, including a similar effect of gM deletion on the BoHV-1 plaques. The authors imply, however, efficient gM-independent, VP22-mediated incorporation of UL49.5 into BoHV-1 Cooper strain virions. This result does not seem to correspond to the the retention of UL49.5 in the ER in the absence of gM that was observed by us.

Our studies on UL49.5 chimeras demonstrate that the N-terminal domain of UL49.5 is sufficient to form a complex with gM as long as it is anchored to the membranes. Nevertheless, the lack of a closely related transmembrane region resulted in both UL49.5 instability (lower steady-state levels) and strong impairment of the complex maturation and trafficking. We were previously able to demonstrate the destabilization of UL49.5 with the TM exchanged to sequences of human Toll-like receptor 2 or CD3δ [34]. Linking the N-terminal domain of BoHV-1-encoded UL49.5 with the homologous TM region from the VZV UL49.5 improved gM maturation and complex release, but still not to the level achieved by the wild-type complex (containing a BoHV-1 N-terminal fragment with BoHV-1 TM). This finding indicates that the sequence of UL49.5 TM can influence the UL49.5/gM processing. One possible explanation could be that this region contains motifs that are important for interactions with gM; alternatively, its sequence and/or structure could also affect conformation of the N-terminal domain. Our structural studies on BoHV-1 and VZV UL49.5 are in progress.

A search for conserved functional motifs in the TM of gM and UL49.5 suggested the presence of GxxxG motifs and glycine zippers in the first, fifth and seventh TM of gM, in addition to the A/GxxxA sequence in the TM of UL49.5 that is conserved in varicelloviruses. Triple leucine substitutions or even a single (A223L) leucine substitution of the gM fifth TM-present G219/A223/G227 residues (GAG/LLL) resulted in impaired UL49.5 binding (despite the presence of intact conserved cysteine residues for the disulfide bridge), potent abrogation of gM maturation and its ER retention. These mutations also had an important functional consequence, as the gM GAG/LLL and A223L mutants failed to counteract the immunomodulatory activity of UL49.5. It is difficult to predict the functional conservation of this particular motif. The sequence from the seventh TM, active in VZV gM [25], has more similarities among the homologues. The G280/G284/A288 mutations analysed in this study seem to impair complex formation and affect the immunomodulatory properties of UL49.5, although only partially. The role of the fifth TM for the biology of VZV gM has not been addressed by Sadaoka *et al.* As the AVMVA sequence in the TM of UL49.5 was not confirmed here as the interaction partner for gM GAG motif, the glycine zipper (potentially in concert with the GGA motif) may contribute to the protein self-interactions, interactions within the lipid bilayer, and, as a consequence, proper folding, as reported for other multimembrane-spanning proteins (recently for the glycine zippers within two TM helices of hepatitis C virus NS4B protein) [29].

METHODS

Cells and viruses

MDBK (ATCC) and MJS cell lines were cultured in RPMI 1640 medium (Sigma-Aldrich), supplemented with 10 % foetal bovine serum (FBS). Bovine KOP-R cells (Collection of Cell Lines in Veterinary Medicine, Federal Research Centre for Virus Diseases of Animals, Insel Riems, Germany)

were cultured in Eagle's minimum essential medium (Sigma-Aldrich) supplemented as above. In this study, BoHV-1 field strain Lam wild-type (WT) or its ΔUL49.5 mutant [10] was used. BoHV-1 (strain Jura) DNA clones as bacterial artificial chromosomes were maintained in *Escherichia coli* DH10B cells [32] and were used in constructing mutant viruses. All viruses were propagated and titrated using MDBK cells.

Generation of mutant viruses

The mutant viruses were generated as follows. The first step was the production of a replication-deficient BoHV-1 strain Jura BAC mutant by introducing the kanamycin resistance Kan^R gene in place of the gM-encoding UL10 sequence and disrupting the essential UL9 gene (the START codon of UL9 was removed) (Fig. 1a,b). Using primers 1 and 2 (Table S1), Kan^R was amplified with Phusion High Fidelity DNA polymerase (Thermo Scientific) from pBluescriptKS (+)rspLKanR (p118) plasmid [32]. Then, 50 nt arms for homologous recombination, flanking the Kan^R sequence, were introduced during a PCR reaction. The Kan^R cassette was electroporated into the arabinose-induced DH10B cells containing the BoHV-1 BAC DNA and pKD46 plasmid encoding the Red recombinase under arabinose-inducible promoter. The recombinant BoHV-1 BAC Kan^R DNA was evaluated by HindIII and HpaI restriction analysis (data not shown) and sequencing. In the second step, the BAC mutant was rescued by replacing the *KanR* gene by versions of the UL10 gene (Fig. 1c), resulting in the recovery of UL9 expression. To construct the ΔgM cassette, a 1276 nt sequence (position 8 3701–8 4977 in BoHV-1 genome, GenBank accession number JX898220) upstream of UL10 and an 831 nt sequence (position 8 5641–8 6472) downstream of UL10 were amplified from BoHV-1 DNA (with primers 3–4 and 5–6, respectively). The obtained fragments were cloned into the EcoRI and SmaI sites of the pUC19 plasmid. A homologous arm upstream of UL10 was recloned from pUC19 into the EcoRI site of pJET1.2 (Thermo Scientific) in order to construct the gMΔtail cassette. A 1440 nt sequence downstream of UL10 (position 8 5032–8 6472), introducing a 54 nt deletion and disrupting the C-terminal domain (predicted by the TMHMM 2.0 program), was amplified from the BoHV-1 genome (with primers 6 and 7). The c-myc tag EQKLISEEDL was introduced at the C-terminus of the UL10 sequence using a combination of primer 6 with primers 8, 9 and 10 and cloned to pJET1.2 into EcoRI and BamHI sites. Using Eco47III and NruI, ΔgM and gMΔtail cassettes were excised from pUC19 and pJET1.2 and co-transfected with BoHV-1 BAC Kan^R DNA into KOP-R cells using the CalPhos Transfection kit (Clontech). The following BoHV-1 mutants were constructed: BoHV-1 ΔgM and BoHV-1 gMΔtail.

Generation of stable MJS cell lines producing UL49.5 and gM variants

Using combinations of primers 11/12 and 11/13 (Table S1), unmodified gM (gMwt) and gMΔtail were amplified from pcDNA-gM-IRES-NLS-GFP plasmid [7] and inserted into the BamHI and HindIII sites of pcDNA3.1/*myc*-His plasmid (Thermo Scientific). Next, c-myc-His-tagged gM variants were recloned into the BamHI/EcoRI sites of pLZRS-IRES-ΔNGFR [7]. The construction of a chimeric UL49.5 variant $BoHV_N$-VZV_{TM} was described previously [34]. To construct a $BoHV_N$-HA_{TM+C} UL49.5, fusion PCR was applied: a sequence coding for the BoHV-1 UL49.5 N-terminal domain was amplified from pcDNA-UL49.5-IRES-NLS-GFP plasmid [4] with primers 16 and 17, and the TM region-encoding sequence was amplified using pFASTBAC plasmid (Thermo Scientific) containing HA H5 gene from a Polish H5N1 isolate [A/swan/Poland/305–135 V08/2006, EpiFluDatabase (http://platform.gisaid.org) accession number EP1156789] and primers 18/19. Joining PCR reactions were subsequently performed with the primers 16 and 19 on mixtures of PCR products from two previous reactions. All PCR reactions were performed using high-fidelity Pwo polymerase (A & A Biotechnology) in conditions recommended by the manufacturer. Using EcoRI and BamHI, constructed sequences of UL49.5 variants were inserted into pLZRS-IRES-GFP plasmid. Using primers 11 and 10, gM-c-myc was amplified by KOD Hot Start DNA polymerase (Novagen) and inserted into pFastBacDUALCMV vector [40]. UL49.5 and gM sequences with substitutions were constructed in pcDNA3-UL49.5-IRES-NLS-GFP and pFastBacDUALCMVgMwt-c-myc, respectively, using the QuikChange Lightning Site-Directed Mutagenesis kit (Agilent Technologies) according to the manufacturer's protocol. Table S1 lists the primers used to introduce mutations. Two PCR reactions were performed in order to construct UL49.5 A65L/A69L (AA/LL). The first PCR reaction introduced a leucine codon at the position corresponding to aa 69 of UL49.5 (primers 28 and 29). The second PCR reaction introduced a leucine codon at the position corresponding to aa 65 of UL49.5, using primers 30 and 31 and pcDNA-UL49.5A69L-IRES-NLS-GFP as a template. Next, UL49.5 variants were inserted into pLZRS-IRES-GFP and gM variants were inserted into pLZRS-IRES-ΔNGFR retrovirus vectors using BamHI and EcoRI sites. The Phoenix Ampho packaging system was used to obtain recombinant retroviruses as described previously [7]. Next, the collected retrovirus-containing supernatants were used for the transduction of MJS cells. The retrovirus-carrying gMwt gene and the MJS stable cell lines UL49.5wt, UL49.5Δtail and UL49.5Δtail gMwt have been described previously [7]. Using a FACSCalibur flow cytometer sorting option (Becton Dickinson), GFP-positive or/and ΔNGFR-positive cells were sorted to obtain cell lines that were at least 95% positive for each marker expression.

Antibodies

Anti-c-myc epitope MAb (clone PL14, Acris Antibodies), goat anti-c-myc PAb (Abcam), or rabbit PAb against 32 C-terminal aa residues of BoHV-1 gM [7] were used to detect gM. BoHV-1 UL49.5 was visualized with rabbit PAb (H11) against a synthetic peptide derived from the N-terminal domain of UL49.5 [7]. Anti-human MHC class I complex MAb (clone W6/32, Santa Cruz Biotechnology) was used in

the flow cytometry. Anti-TAP1 monoclonal antibody (MAb 143.5) was kindly provided by R. Tampé (Institute of Biochemistry, The Johann Wolfgang Goethe University, Frankfurt, Germany) and anti-TAP2 MAb 435.3 was a kind gift from P. van Endert (INSERM U25, Institute Necker, Paris, France). To visualize the TGN, anti-γ-adaptin MAb (clone 100/3, Sigma) was used. To visualize ER, Alexa 633-conjugated concanavalin A (ConA) was used (Thermo-Molecular Probes). To visualize the plasma membrane, anti-β-catenin MAb was used (Sigma-Aldrich). Early endosomes were stained with anti-EEA1 MAb (BD Biosciences). β-actin (detected by rabbit PAb from Novus Biologicals) or β-catenin (detected by rabbit PAb from Santa Cruz Biotechnology) were used as loading controls in immunoblotting.

Immunoblotting and immunoprecipitation

For immunoblotting and immunoprecipitation, the collected cells were lysed in a lysis buffer containing 0.5 % (w/v) Nonidet-P40 in 50 mM Tris-HCl pH 7.5, 5 mM $MgCl_2$, or in the whole cell-lysing CelLytic M buffer (Sigma-Aldrich); all buffers were supplemented with the Complete Mini Protease Inhibitor Cocktail (Roche). Next, cell lysates were analysed by SDS-PAGE (for non-reducing conditions in the absence of 5 % β-mercaptoethanol) and immunoblotting directly or incubated with anti-gM or anti-c-myc MAb together with Protein-A Sepharose beads (Sigma Aldrich) to isolate protein complexes. For the analysis of N-linked glycosylation, equivalent amounts of cell lysates were incubated with endo-β-N-acetylglucosaminidase H (EndoH; New England Biolabs) or peptide : N-glycosidase F (PNGaseF; New England Biolabs) according to the manufacturer's conditions. Cell lysates and immunoprecipitated proteins were separated in SDS-PAGE and immunoblotted as described before [7].

Immunofluorescence

Cells were grown on microcover glass. Where indicated, they were infected with BoHV-1 variants at a multiplicity of infection m.o.i. of 0.6 for 14 h. Next, cells were fixed with 4 % paraformaldehyde in PBS and permeabilized with 0.2 % (w/v) Triton X-100 in PBS for 7 min. After washing with PBS, cells were incubated with H11 anti-BoHV-1 UL49.5 antibodies (1 : 5000) or goat/mouse anti-c-myc antibodies (1 : 1000), or anti-gM antibodies (1 : 5000) in combination with anti-γ-adaptin MAb (1 : 500) (for TGN staining) for 1 h. After washing, cells were incubated with suitable secondary antibodies; for ER staining, ConA-Alexa 633 conjugate was added (1 : 1000). UL49.5 and gM were visualized using Alexa 546-conjugated donkey anti-rabbit IgG (1 : 1000; Thermo-Molecular Probes), while TGN marker and gM-c-myc were detected with Alexa 405-conjugated donkey anti-mouse IgG (1 : 500; Thermo-Molecular Probes). gM stained with goat anti-c-myc antibody was detected by Alexa 633-conjugated donkey anti-goat IgG (1 : 1000; Thermo-Molecular Probes). The stained cells were analysed using a Leica TCS SP8X confocal laser scanning microscope. The degree of co-localization was analysed using Leica Application Suite X software and quantified using Pearson's correlation coefficient.

Flow cytometry

Cell surface expression of specific molecules was determined by indirect immunofluorescence using primary antibodies as indicated and, as a second step, Alexa 633-conjugated goat anti-mouse or donkey anti-rabbit IgG (1 : 1000; Thermo-Molecular Probes). MJS cells were stained as above or only with Alexa 633-IgG as controls. Cells were analysed using a FACSCalibur flow cytometer (Becton Dickinson) and CellQuest Pro software.

Funding information
This study was supported by grants POMOST/2010/2–7 from the Foundation for Polish Science and UMO-2014/14/E/NZ6/00164 from the Polish National Science Center to A. D. L.

Acknowledgements
We thank Beata Gromadzka, Department of Recombinant Vaccines, Intercollegiate Faculty of Biotechnology, UG and MUG for sharing influenza haemagglutinin plasmid. The authors would like to thank Ana I. Costa, Medical Microbiology, University Medical Center Utrecht, for assisting with the preparation of the manuscript.

Conflicts of interest
The authors declare that there are no conflicts of interest.

References
1. **Gibbs EPJ, Rweyemamu MM.** Bovine herpesviruses. Part 1: bovine herpesvirus 1. *Vet Bull* 1977;47:317–343.
2. **Griffin BD, Verweij MC, Wiertz EJ.** Herpesviruses and immunity: the art of evasion. *Vet Microbiol* 2010;143:89–100.
3. **Levings RL, Roth JA.** Immunity to bovine herpesvirus 1: II. Adaptive immunity and vaccinology. *Anim Health Res Rev* 2013;14:103–123.
4. **Koppers-Lalic D, Reits EA, Ressing ME, Lipinska AD, Abele R *et al.*** Varicelloviruses avoid T cell recognition by UL49.5-mediated inactivation of the transporter associated with antigen processing. *Proc Natl Acad Sci USA* 2005;102:5144–5149.
5. **Liang X, Tang M, Manns B, Babiuk LA, Zamb TJ.** Identification and deletion mutagenesis of the bovine herpesvirus 1 dUTPase gene and a gene homologous to herpes simplex virus UL49.5. *Virology* 1993;195:42–50.
6. **Liang X, Chow B, Raggo C, Babiuk LA.** Bovine herpesvirus 1 UL49.5 homolog gene encodes a novel viral envelope protein that forms a disulfide-linked complex with a second virion structural protein. *J Virol* 1996;70:1448–1454.
7. **Lipińska AD, Koppers-Lalic D, Rychłowski M, Admiraal P, Rijsewijk FA *et al.*** Bovine herpesvirus 1 UL49.5 protein inhibits the transporter associated with antigen processing despite complex formation with glycoprotein M. *J Virol* 2006;80:5822–5832.
8. **Wu SX, Zhu XP, Letchworth GJ.** Bovine herpesvirus 1 glycoprotein M forms a disulfide-linked heterodimer with the U(L)49.5 protein. *J Virol* 1998;72:3029–3036.
9. **König P, Giesow K, Keil GM.** Glycoprotein M of bovine herpesvirus 1 (BHV-1) is nonessential for replication in cell culture and is involved in inhibition of bovine respiratory syncytial virus F protein induced syncytium formation in recombinant BHV-1 infected cells. *Vet Microbiol* 2002;86:37–49.
10. **Koppers-Lalic D, Verweij MC, Lipińska AD, Wang Y, Quinten E *et al.*** Varicellovirus UL49.5 proteins differentially affect the function of the transporter associated with antigen processing, TAP. *PLoS Pathog* 2008;4:e1000080.
11. **Wei H, He J, Paulsen DB, Chowdhury SI.** Bovine herpesvirus type 1 (BHV-1) mutant lacking U(L) 49.5 luminal domain residues 30–

32 and cytoplasmic tail residues 80-96 induces more rapid onset of virus neutralizing antibody and cellular immune responses in calves than the wild-type strain Cooper. *Vet Immunol Immunopathol* 2012;147:223–229.

12. **Kawabata A, Jasirwan C, Yamanishi K, Mori Y.** Human herpesvirus 6 glycoprotein M is essential for virus growth and requires glycoprotein N for its maturation. *Virology* 2012;429:21–28.
13. **Koyano S, Mar EC, Stamey FR, Inoue N.** Glycoproteins M and N of human herpesvirus 8 form a complex and inhibit cell fusion. *J Gen Virol* 2003;84:1485–1491.
14. **Lake CM, Hutt-Fletcher LM.** Epstein-Barr virus that lacks glycoprotein gN is impaired in assembly and infection. *J Virol* 2000;74: 11162–11172.
15. **Rudolph J, Seyboldt C, Granzow H, Osterrieder N.** The gene 10 (UL49.5) product of equine herpesvirus 1 is necessary and sufficient for functional processing of glycoprotein M. *J Virol* 2002;76: 2952–2963.
16. **Crump CM, Bruun B, Bell S, Pomeranz LE, Minson T *et al.*** Alphaherpesvirus glycoprotein M causes the relocalization of plasma membrane proteins. *J Gen Virol* 2004;85:3517–3527.
17. **Jöns A, Dijkstra JM, Mettenleiter TC.** Glycoproteins M and N of pseudorabies virus form a disulfide-linked complex. *J Virol* 1998; 72:550–557.
18. **Kopp M, Granzow H, Fuchs W, Klupp B, Mettenleiter TC.** Simultaneous deletion of pseudorabies virus tegument protein UL11 and glycoprotein M severely impairs secondary envelopment. *J Virol* 2004;78:3024–3034.
19. **Osterrieder N, Neubauer A, Brandmuller C, Braun B, Kaaden OR *et al.*** The equine herpesvirus 1 glycoprotein gp21/22a, the herpes simplex virus type 1 gM homolog, is involved in virus penetration and cell-to-cell spread of virions. *J Virol* 1996;70:4110–4115.
20. **Yamagishi Y, Sadaoka T, Yoshii H, Somboonthum P, Imazawa T *et al.*** Varicella-zoster virus glycoprotein M homolog is glycosylated, is expressed on the viral envelope, and functions in virus cell-to-cell spread. *J Virol* 2008;82:795–804.
21. **Ziegler C, Just FT, Lischewski A, Elbers K, Neubauer A.** A glycoprotein M-deleted equid herpesvirus 4 is severely impaired in virus egress and cell-to-cell spread. *J Gen Virol* 2005;86:11–21.
22. **Mach M, Kropff B, dal Monte P, Britt W.** Complex formation by human cytomegalovirus glycoproteins M (gpUL100) and N (gpUL73). *J Virol* 2000;74:11881–11892.
23. **Mach M, Kropff B, Kryzaniak M, Britt W.** Complex formation by glycoproteins M and N of human cytomegalovirus: structural and functional aspects. *J Virol* 2005;79:2160–2170.
24. **Striebinger H, Funk C, Raschbichler V, Bailer SM.** Subcellular trafficking and functional relationship of the HSV-1 glycoproteins N and M. *Viruses* 2016;8:83.
25. **Sadaoka T, Yanagi T, Yamanishi K, Mori Y.** Characterization of the varicella-zoster virus ORF50 gene, which encodes glycoprotein M. *J Virol* 2010;84:3488–3502.
26. **Hacke M, Björkholm P, Hellwig A, Himmels P, Ruiz de Almodóvar C *et al.*** Inhibition of Ebola virus glycoprotein-mediated cytotoxicity by targeting its transmembrane domain and cholesterol. *Nat Commun* 2015;6:7688.
27. **Falson P, Bartosch B, Alsaleh K, Tews BA, Loquet A *et al.*** Hepatitis C virus envelope glycoprotein E1 forms trimers at the surface of the virion. *J Virol* 2015;89:10333–10346.
28. **Teese MG, Langosch D.** Role of GxxxG motifs in transmembrane domain interactions. *Biochemistry* 2015;54:5125–5135.
29. **Paul D, Madan V, Ramirez O, Bencun M, Stoeck IK *et al.*** Glycine zipper motifs in hepatitis C virus nonstructural protein 4B are required for the establishment of viral replication organelles. *J Virol* 2018;92:e01890–17.
30. **Nishimura N, Balch WE.** A di-acidic signal required for selective export from the endoplasmic reticulum. *Science* 1997;277:556–558.
31. **Parmar HB, Barry C, Duncan R.** Polybasic trafficking signal mediates golgi export, ER retention or ER export and retrieval based on membrane-proximity. *PLoS One* 2014;9:e94194.
32. **Gabev E, Tobler K, Abril C, Hilbe M, Senn C *et al.*** Glycoprotein D of bovine herpesvirus 5 (BoHV-5) confers an extended host range to BoHV-1 but does not contribute to invasion of the brain. *J Virol* 2010;84:5583–5593.
33. **Robinson KE, Meers J, Gravel JL, McCarthy FM, Mahony TJ.** The essential and non-essential genes of Bovine herpesvirus 1. *J Gen Virol* 2008;89:2851–2863.
34. **Verweij MC, Lipińska AD, Koppers-Lalic D, Quinten E, Funke J *et al.*** Structural and functional analysis of the TAP-inhibiting UL49.5 proteins of varicelloviruses. *Mol Immunol* 2011;48:2038–2051.
35. **Geva Y, Schuldiner M.** The back and forth of cargo exit from the endoplasmic reticulum. *Curr Biol* 2014;24:R130–R136.
36. **Michelsen K, Yuan H, Schwappach B.** Hide and run. Arginine-based endoplasmic-reticulum-sorting motifs in the assembly of heteromultimeric membrane proteins. *EMBO Rep* 2005;6:717–722.
37. **El Kasmi I, Lippé R.** Herpes simplex virus 1 gN partners with gM to modulate the viral fusion machinery. *J Virol* 2015;89:2313–2323.
38. **Striebinger H, Zhang J, Ott M, Funk C, Radtke K *et al.*** Subcellular trafficking and functional importance of herpes simplex virus type 1 glycoprotein M domains. *J Gen Virol* 2015;96:3313–3325.
39. **Pannhorst K, Wei H, Yezid H, He J, Chowdhury SI.** Bovine herpesvirus 1 U_L49.5 interacts with gM and VP22 to ensure virus cell-to-cell spread and virion incorporation: novel role for VP22 in gM-independent U_L49.5 virion incorporation. *J Virol* 2018;92:e00240-18–18.
40. **Grabowska AK, Lipińska AD, Rohde J, Szewczyk B, Bienkowska-Szewczyk K *et al.*** New baculovirus recombinants expressing Pseudorabies virus (PRV) glycoproteins protect mice against lethal challenge infection. *Vaccine* 2009;27:3584–3591.